

Geochemical Characteristics Of The Trace Elements And Heavy Metals In The Sequences In Gachsaran Formation, West Of Iran

Sakhavati Behnam^{*1}, Yousefirad Mostafa², Anita Yaghotipoor³

¹Department of Geology, Faculty of Earth Sciences, Payame Noor University, Tehran, Iran

²Department of Geomechanic engineering, Faculty of earth science engineering, Arak University of Technology, Iran

³College of Agriculture, Razi University, Kermanshah, Iran

*Corresponding author

Sakhavati Behnam, Department of Geology, Faculty of Earth Sciences, Payame Noor University, Tehran, Iran

Submitted: 17 Apr 2022; Accepted: 28 Apr 2022; Published: 04 May 2022

Citation: Sakhavati Behnam., Yousefirad Mostafa., Anita Yaghotipoor. (2022). Geochemical Characteristics Of The Trace Elements And Heavy Metals In The Sequences In Gachsaran Formation, West Of Iran. *Petro Chem Indus Intern*, 5(2), 87-99.

Abstract

In the present study, the geochemical characteristics of sequences of the Gachsaran Formation, located in the west of Kermanshah province, Iran - Iraq border zones, were studied. In order to determine the concentration of the elements, the XRF and ICP-mass techniques were employed, and the XRD technique was used to identify the mineralogical composition and finally, the evaluation of the level of pollution caused by these elements were carried out using statistical and pollution index software.

The results illuminated that the concentrations of CaO, MgO, TiO₂, and concentrations of two elements, i.e., Cd and Sb were higher than their mean values in the earth's crust. Based on the CF pollution index, the elements of Cd and Sb with the values of 1.52 and 2 show the moderate contamination. Enrichment factor (EF) revealed moderate contamination for Cs (2.46), Ga (3.86), Rb (2) and Ti (2.35). This index showed the high pollution and anthropogenic origin for Ti (8), Cd (10.41), U (11.26) and Sb (13.43). The results of the correlation between the elements indicated the presence of positive and significant correlation between Cs, Hf, La, Nb, Nd, Rb, Sc, Sm, Ta, Tb, Th, Tl, W, Y, Yb, and Zr. There was no positive and significant correlation between U and none of the elements. Three elements of Sb, U, and Cd showed a negative correlation with most of the studied elements. According to the results of cluster analysis, three separate groups were obtained so that each of Ti and Fe was classified as separate groups and Fe showed the highest difference in comparison with other elements. Based on the results of the Principal Component Analysis (PCA), the highest effect was related to the elements of Cs, Hf, La, Nb, Rb, Sc, Sm, Tb, Th, Tl, W, Y, Yb, Zr; Fe in the first Component, Sb, Cd in second component and U in the third component.

Keywords: Geochemistry, Gachsaran Formation, Earth's trace elements, Heavy metals, Pollution index.

Introduction

The Gachsaran Formation deposits, called Lower Fars Formation (Miocene) by Cox in Iran, is the most important cap rocks of the Zagros hydrocarbon basin, and its equivalents, i.e., Fatha Formation in Iraq and Dam Formation in the Persian Gulf countries have outcrop in most parts of the Middle East with significant extent [1].

The sediments in Iran were first studied by [2]. Then, other researchers including, have conducted studies on the sediments [3-9]. There is no complete type section for Gachsaran Formation in the earth's surface and it mainly consists of intermittent and sometimes repetitive sequences of evaporate, carbonate rocks and marl. Its type section in consolidated form in the wells of the oil fields of Iran consists of 7 sections with a total thickness of about 1,600 m [10].

These sequences are soft erosion and soluble and its widespread expansion and its equivalent formations are significant in many Middle Eastern countries. Identification of chemical facies variations and possible contamination caused by the concentration of contaminant chemicals in these sequences seems to be essential due to the high solubility properties of evaporate and carbonate units in aquatic environments.

Contaminants are usually deposited in sediments accumulated in rivers and beaches to be the bedrock of rivers, which can be transmitters of pollution. Strategies to prevent and reduce pollution through examining the geochemical properties of river bed rocks, if they lead to the identification of chemical contaminants, can be

very easy and low-cost, compared to encountering them in deposits downstream of the waterways and coasts. Even if the moderate level of chemical contaminants in bedrock are identified, which may be exacerbated by human factors, environmental precautions can be considered to reduce or eliminate these effects downstream.

In recent years, heavy metal contamination in the aquatic environment has become a global problem [11]. Due to the toxic potential of these metals and their ability to bioaccumulate in aquatic ecosystems, the level of metal contamination in these areas has raised more public concern in recent years [12, 13]. Sources of heavy metal contamination in aquatic environments are industrial waste and mining [14]. Mining operations that involve the extraction of minerals and ores beneath the surface are associated with environmental destruction, environmental pollution and related diseases, resulting from the dispersal of some trace elements in the surrounding environment [15, 16]. Natural sources of heavy metals may also include weathering, dissolution of bedrock minerals and soils [17, 18]. Natural sources of heavy metals may also include weathering, dissolution of bedrock minerals and soils [17, 18]. Aquatic ecosystems such as rivers are the sinks for contaminants, probably because rivers are open ecosystems, they are more vulnerable to anthropogenic pollution [19, 20]. Finally, river sediments are used as primary sinks for contaminants, including heavy metals [21]. The sediments are usually a combination of different components including different minerals as well as organic matter that can play a significant role in transferring contaminants in aquatic systems and the interactions between water and sediments [22]. One of the areas that, so far, have not been studied is the sequence of the Gachsaran Formation in the Emamhasan stratigraphical section in western Iran. These studies are important for understanding the geochemical nature and possible contamination of these sequences along the Cham e Hassan River.

Geographical location and geological characteristics of the area

The study area is located at the southern domain of the Imam Hassan anticline, located in 156 km west of Kermanshah and 17 km, the Iran-Iraq border, with a mean latitude of 34°51'22" N and latitude of 45°48'44" (Figure 1).

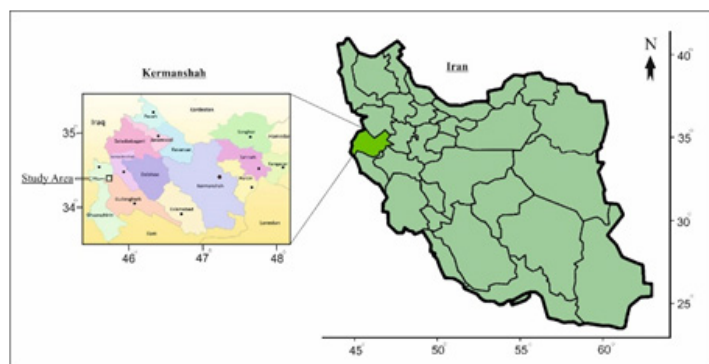


Figure 1: Geographical location of the study area

The study area is located in the Sedimentary basin of western Lorestan. The lithostratigraphic units that exist in this region are related to Mesozoic (Cretaceous) which mainly consists of limestone, shale and has located under the Tertiary Formation. The Tertiary rock units that have outcrop in the upper horizons can also be considered to have limestone, shale, sandstone, and conglomerates, in which the limestones of this group are cliff maker.

Quaternary sedimentary units have deposited in the plains and low-lying areas and on the riverside. The oldest rocks of the Sarpol- E Zahab range belong to the Cretaceous and include Ilam and Gurpi Formation. Pabdeh, Asmari, Gachsaran, Aghajari and Bakhtiari are also highest stone horizons in the range of Sarpol- E Zahab (geological map of Sarpol- E Zahab. 2013) (Figure 2). The geological location of depositional sequences of the Gachsaran Formation and the sampling site consist of sedimentary cycles, including frequent and repeated sequences of evaporite deposits, carbonate and clastic rocks (thickness of 445.6 m), consisting of 79 m gypsum (18%), 132.5 m various types of dolomitic, silty and marly limestones (30%) and 306.6 m colorful marls (52%) which are predominantly red, green and, with a less extent, gray and yellow (Figure 3).

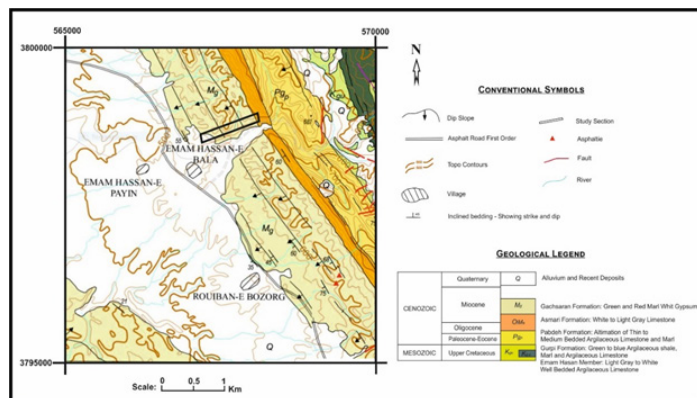


Figure 2: Geological map of the study area (Modified from Geological map of Sarpol- E Zahab, 1:50000, National Iranian Oil Company, 2013)



Figure 3: Stratigraphic position and the upper and lower boundaries of the Gachsaran Formation in the Emamhasan section, the east view.

Materials and Method

Sampling, in a condensed form, was conducted on 105 rocks and weathered sediments of the Gachsaran Formation in Imamhassan stratigraphic section in a path perpendicular to layers from the end of Asmari Formation to the beginning of Aghajari Formation and parallel to Imamhassan Cham River path based on lithological changes (Figure 3). Sediment samples were collected from a depth of 20 cm. The samples were placed in Polyethylene bags, then transferred to the Laboratory of Applied Research Center of Geology of Iran for XRD analysis and elemental concentration determination by ICP-mass. The oxides in the samples were also analyzed by XRF analysis at the laboratory of the Geological Survey of Iran.

The results of the analysis are compared with the contamination classification index factors included Enrichment Factor, Contamination Factor and Geoaccumulation Index, then multivariate statistical analysis that provides important information for better understanding the complex dynamics of pollutants in the aquatic ecosystem were carried out [23]. Multivariate analysis including Pearson correlation, cluster analysis (CA) and principal component analysis (PCA) were used to determine heavy metal sources. Pearson correlation analysis was employed to determine the interactions between heavy metals in sediments and Cluster Analysis (CA) was used to explain the spatial distribution of heavy metals in sediments as well as to classify elements with different sources based on their similarities and identification of homogeneous variables that have similar characteristics [24-26]. Data were analyzed using the Kolmogorov-Smirnov test and SPSS software version 17.

Table 1: Enrichment Factor (EF) of Trace metals in Imamhassan section

Sample	Ti	CS	Ga	Hf	La	Nb	Nd	Rb	Sb	Sc	Sm	Ta	Tb	Th	Tl	U	W	Y	Yb	Zr	Cd	
1	ND	ND	ND	ND	ND	ND	ND	ND	ND	ND	ND	ND	ND	ND	ND	ND	ND	ND	ND	ND	ND	ND
2	19.75	3.14	8.93	1.45	3.89	2.11	1.69	3.53	39.29	1.24	1.70	1.48	1.49	1.33	5.96	40.74	3.11	1.37	1.56	1.27	31.49	
3	42.32	2.99	27.74	2.30	4.35	2.58	2.23	5.30	27.63	2.07	2.61	1.31	2.63	1.62	8.94	131.99	4.02	2.25	2.52	1.50	21.01	
4	1.60	2.43	1.14	1.62	0.91	0.62	0.87	1.26	2.78	0.60	0.79	0.15	0.69	0.88	1.14	1.37	0.75	0.61	0.73	1.03	1.49	
5	0.72	2.98	1.11	1.77	0.92	0.72	0.76	1.42	1.85	0.67	0.75	0.14	0.68	0.91	1.05	0.90	1.06	0.62	0.83	1.18	1.34	
6	5.64	2.15	1.91	1.54	1.87	1.77	1.60	1.67	8.75	0.73	1.61	0.17	1.47	0.96	1.49	2.54	1.44	1.50	1.28	1.01	3.35	
7	6.16	2.27	2.07	1.94	2.94	1.24	2.48	1.86	12.66	0.87	2.29	0.44	1.94	1.30	1.63	2.21	1.51	1.65	1.63	1.57	4.26	
8	2.21	5.55	2.76	3.88	2.64	1.70	2.61	2.91	5.96	1.62	2.13	0.55	1.92	2.52	2.47	2.33	1.78	1.75	2.17	2.89	1.75	
9	2.18	1.92	1.00	0.96	0.83	0.54	0.79	1.30	8.66	0.53	1.01	0.23	0.63	0.73	1.00	1.53	0.67	0.70	0.78	0.82	1.30	
10	38.09	2.54	11.71	2.28	1.52	2.11	0.81	3.96	50.86	1.34	0.92	4.37	2.24	0.97	8.94	1.37	3.84	0.87	0.67	1.82	20.12	
11	1.61	2.03	1.38	1.47	1.01	0.80	0.85	1.28	4.84	0.68	0.84	0.26	0.79	0.80	1.23	2.59	0.98	0.90	0.90	1.18	5.13	
12	0.75	2.83	1.39	1.31	1.27	0.77	1.30	1.51	3.84	0.94	0.95	0.50	0.79	1.36	1.33	1.18	0.83	0.70	0.89	0.93	1.47	
13	3.49	1.86	1.07	1.37	1.40	0.90	0.96	1.80	6.60	0.99	0.89	0.61	0.71	0.89	1.05	5.76	0.89	0.84	0.92	1.03	4.93	
14	3.14	2.32	1.20	1.14	1.05	0.70	0.90	1.30	4.61	0.72	0.83	0.36	0.76	0.84	0.94	2.02	0.87	0.68	0.76	0.80	1.49	
15	0.95	2.77	1.17	1.49	0.97	0.70	0.94	1.41	2.08	0.68	0.76	0.28	0.64	1.02	1.04	0.70	0.79	0.57	0.76	0.99	0.97	
16	0.98	2.38	1.08	1.32	0.83	0.68	0.74	1.20	2.66	0.61	0.73	0.36	0.60	0.96	1.04	0.67	0.73	0.54	0.65	1.06	0.62	
17	1.15	1.04	0.81	1.01	1.08	0.47	1.03	0.75	2.88	0.48	0.98	0.14	0.73	0.76	0.67	0.51	0.76	0.61	0.69	0.74	1.04	
18	ND	ND	ND	ND	ND	ND	ND	ND	ND	ND	ND	ND	ND	ND	ND	ND	ND	ND	ND	ND	ND	ND
19	1.06	2.01	1.04	1.31	1.00	0.65	0.84	1.11	2.31	0.68	0.80	0.31	0.78	0.91	0.97	1.07	0.68	0.65	0.85	0.92	1.03	
20	7.26	1.05	1.90	1.08	2.19	0.83	1.67	1.58	53.48	0.82	1.45	0.38	1.44	0.77	1.49	3.1	1.45	1.19	1.01	0.79	84.51	
Mean	8	2.46	3.86	1.62	1.7	1.10	1.28	2.0	13.43	0.90	1.22	0.67	1.16	1.09	2.35	11.2	1.45	1.00	1.09	1.20	10.41	

Results and Discussion

Pollution Indices

Pollution indices investigated in this research include Enrichment Factor (EF), Contamination Factor (CF) and Geoaccumulation Index (Igeo).

Enrichment Factor (EF)

The enrichment factor (EF) calculation is used to quantify the contribution of human resources in heavy metal concentrations [27]. The enrichment factor is calculated by the following formula:

$$EF = \frac{[(Metal/Fe)_{Sample}]}{[(Metal/Fe)_{Background}]}$$

This formula refers to the ratio of contaminations of elements and iron in sediments and earth's crust

This paper uses the contamination rating system proposed by in which if the enrichment factor is less than 2, it means that the sediments are lack of contamination or they have minimal contamination; EF = 2-5 shows moderate contamination; EF = 5-20 indicates significant contamination; EF = 20-40 indicates very high contamination, and EF > 40 indicates extremely high enrichment [28, 29].

The following values (Table 1) were obtained for the contamination ratings using the enrichment factor (EF) in the sequences of Imamhassan stratigraphical section.

(Table 1) shows the results of the enrichment factor (EF) of the studied elements. These results show that Hf (1.62), La (1.7), Nb (1.10), Nd (1.28), Sc (0.90), Sm (1.22), Ta (0.67), Tb (1.16), Th (1.09), W (1.45), Y (1), Yb (1.09) and Zr (1.20) were lack of contamination or with minimal contamination based on this index [28, 29]. According to studies, elements with (EF) less than 2 have no human origin but they have an entrance from natural processes [30-32]. The enrichment factor (EF) for Cs (2.46), Ga (3.86), Rb (2) and Tl (2.35) showed moderate contamination. This index for

Ti (8), Cd (10.41), U (26.11) and Sb (13.43) showed significant contamination based on contamination classification[28-29]. According to, elements with EF greater than 2 indicate that these elements have probably anthropogenic origin [30-32]. In this study, Cs (2.46), Ga (3.86), Rb (2) and Tl (2.35) showed moderate contamination. In the case of Ti (8), Cd (10.41), U (26/11) and Sb (13.43), the indices have EF greater than 2 and have an anthropogenic origin.

Contamination Factor (CF)

Contamination factor (CF) is calculated by the following equation:

$$CF = C_m \text{ Sample} / C_m \text{ Background}$$

Where C_m Sample is the metal concentration in sediments and C_m Background shows concentration in the background that the metal content is in the average of shale [33]. According to the classification, contamination levels in sediments using this index are as follows [34]:

$1 < CF < 3$ = low contamination, $3 \leq CF < 6$ = medium contamination, $CF \geq 6$ = significant contamination and $CF > 6$ means very high contamination.

The following values (Table 2) were obtained in the contamination ranking using the contamination index (CF) in the sequences of the Imamhassan stratigraphical section.

Table 2. The contamination factors (CF) of Trace metals in Emamhasan section

Sample	Ti	Cs	Ga	Hf	La	Nb	Nd	Rb	Sb	Sc	Sm	Ta	Tb	Th	Tl	U	W	Y	Yb	Zr	Fe	Cd
1	0.73	0.06	0.29	0.04	0.05	0.82	0.03	0.08	1.91	0.03	0.02	0.03	0.005	0.02	0.22	0.27	0.11	0.017	0.02	0.03	ND	2.30
2	0.73	0.11	0.33	0.05	0.14	0.078	0.06	0.13	1.46	0.04	0.06	0.05	0.005	0.04	0.22	1.51	0.11	0.051	0.058	0.04	0.03	1.15
3	1.05	0.07	0.68	0.05	0.10	0.06	0.05	0.13	0.68	0.05	0.06	0.03	0.006	0.04	0.22	3.27	0.09	0.055	0.06	0.03	0.02	0.50
4	1.05	1.60	0.74	1.06	0.59	0.40	0.57	0.82	1.83	0.39	0.51	0.09	0.04	0.57	0.74	0.90	0.49	0.40	0.47	0.68	0.65	1.00
5	0.52	2.18	0.81	1.29	0.67	0.52	0.55	1.03	1.35	0.49	0.54	0.10	0.05	0.66	0.76	0.65	0.77	0.45	0.61	0.86	0.73	1.00
6	0.84	0.32	0.28	0.22	0.27	0.26	0.23	0.24	1.30	0.10	0.23	0.02	0.02	0.14	0.22	0.37	0.21	0.22	0.19	0.15	0.14	0.50
7	0.84	0.30	0.28	0.26	0.40	0.16	0.33	0.25	1.73	0.11	0.31	0.06	0.02	0.17	0.22	0.30	0.20	0.22	0.22	0.21	0.13	0.60
8	0.63	1.58	0.78	1.10	0.75	0.48	0.74	0.83	1.70	0.46	0.60	0.15	0.05	0.72	0.70	0.66	0.50	0.50	0.62	0.82	0.28	0.50
9	0.84	0.73	0.38	0.37	0.32	0.20	0.30	0.49	3.33	0.20	0.38	0.088	0.024	0.27	0.38	0.59	0.25	0.27	0.29	0.31	0.38	0.50
10	0.94	0.06	0.29	0.05	0.03	0.05	0.02	0.09	1.26	0.03	0.02	0.10	0.005	0.02	0.22	0.03	0.09	0.021	0.01	0.04	0.02	0.50
11	0.42	0.52	0.35	0.38	0.26	0.20	0.22	0.33	1.26	0.17	0.21	0.06	0.02	0.20	0.32	0.67	0.25	0.236	0.23	0.30	0.26	1.35
12	0.42	1.57	0.77	0.72	0.71	0.42	0.72	0.84	2.14	0.52	0.52	0.27	0.04	0.75	0.74	0.66	0.46	0.38	0.49	0.51	0.55	0.80
13	0.73	0.39	0.22	0.28	0.29	0.19	0.20	0.37	1.39	0.20	0.18	0.12	0.01	0.18	0.22	1.21	0.18	0.17	0.19	0.21	0.21	1.05
14	1.05	0.77	0.40	0.38	0.35	0.23	0.30	0.43	1.54	0.24	0.27	0.11	0.025	0.28	0.31	0.67	0.29	0.22	0.25	0.26	0.33	0.50
15	0.84	2.44	1.02	1.31	0.85	0.61	0.83	1.24	1.83	0.59	0.66	0.24	0.05	0.90	0.92	0.61	0.69	0.50	0.67	0.87	0.88	0.85
16	0.84	2.04	0.92	1.12	0.70	0.57	0.63	1.03	2.28	0.52	0.62	0.30	0.05	0.82	0.89	0.57	0.625	0.46	0.55	0.91	0.85	0.55
17	0.94	0.85	0.66	0.82	0.88	0.38	0.84	0.61	2.36	0.39	0.80	0.11	0.05	0.62	0.552	0.42	0.62	0.50	0.56	0.60	0.81	0.85
18	0.841	0.03	0.12	0.03	0.02	0.06	0.01	0.20	1.26	0.059	0.01	0.08	0.005	0.014	0.22	0.04	0.073	0.01	0.016	0.02	ND	0.50
19	0.73	1.39	0.72	0.91	0.69	0.45	0.58	0.77	1.60	0.47	0.55	0.21	0.054	0.63	0.67	0.74	0.46	0.45	0.59	0.64	0.69	0.70
20	1.26	0.18	0.32	0.18	0.38	0.14	0.29	0.27	9.30	0.14	0.25	0.06	0.025	0.13	0.25	0.54	0.25	0.20	0.17	0.13	0.17	14.7
Mean	0.81	0.86	0.52	0.53	0.42	0.31	0.37	0.51	2.08	0.26	0.34	0.11	0.03	0.36	0.45	0.73	0.34	0.27	0.31	0.38	0.40	1.52

According to the results presented in (Table 2) and according to the classification of contamination factor (CF) by (Hakanson 1980), Ti (0.81), Cs (0.86), Ga (0.52), Hf (0.53), La (0.42), Nb (0.31), Nd (0.37), Rb (0.51), Sc (0.26), Sm (0.34), Ta (0.11), Tb (0.03), Th

(0.36), Tl (0.45), U (0.73), W (0.73), Y (0.27), Yb (0.31), Zr (0.38) and Fe (0.4) show low levels of contamination. Whereas, Cd and Sb show moderate contamination with values of (1.52) and (2).

Geoaccumulation Index (Igeo)

The Geoaccumulation Index (Igeo) was introduced by (Muller) to evaluate the contamination in sediments and crust. This index is expressed by the following formula:

$$I_{geo} = \log_2 (C_n / 1.5 B_n)$$

Where C_n is the concentration of the element in the sediments and B_n is the geochemical background value and the constant of 1.5 is the underlying correction index introduced to reduce the effects of lithogenic changes. According to, $I_{geo} \leq 0$ is

indicative of lack of contamination; $0 < I_{geo} < 1$ shows “lack of contamination” to “moderate contamination”; $1 < I_{geo} < 2$ indicates the moderate contamination; $2 < I_{geo} < 3$ indicates the moderate to heavy contamination; $3 < I_{geo} < 4$ shows the heavy contamination; $4 < I_{geo} < 5$ indicates the heavy to extreme contamination; $I_{geo} \geq 5$ reveals the extreme contamination [35].

The following values were obtained in the ranking of the contamination using the Igeo index sequences of the Imamhassan stratigraphical section (Table 3).

Table 3: Geoaccumulation indices (Igeo) of trace metals in Imamhassan section

Sample	Ti	Cs	Ga	Hf	La	Nb	Nd	Rb	Sb	Sc	Sm	Ta	Tb	Th	Tl	U	W	Y	Yb	Zr	Fe	Cd
1	0.61	0.02	0.15	0.03	0.01	1.00	0.03	0.04	0.17	0.04	0.01	0.06	0.03	0.01	0.05	0.13	0.07	0.01	0.02	0.02	ND	1.02
2	0.61	0.05	0.18	0.04	0.03	0.10	0.05	0.06	0.13	0.05	0.04	0.09	0.03	0.03	0.05	0.74	0.06	0.04	0.04	0.03	0.03	0.51
3	0.87	0.03	0.36	0.04	0.02	0.08	0.04	0.06	0.06	0.06	0.04	0.05	0.04	0.02	0.05	1.60	0.06	0.05	0.05	0.03	0.02	0.22
4	0.87	0.64	0.39	0.76	0.13	0.49	0.45	0.36	0.16	0.45	0.32	0.16	0.27	0.31	0.16	0.44	0.27	0.34	0.37	0.47	0.52	0.44
5	0.43	0.87	0.43	0.93	0.15	0.64	0.43	0.44	0.12	0.55	0.34	0.17	0.30	0.36	0.16	0.32	0.43	0.39	0.47	0.60	0.58	0.44
6	0.69	0.13	0.15	0.16	0.06	0.32	0.19	0.11	0.12	0.12	0.15	0.04	0.13	0.08	0.05	0.18	0.12	0.19	0.15	0.10	0.12	0.22
7	0.69	0.12	0.15	0.19	0.09	0.21	0.26	0.11	0.15	0.13	0.20	0.10	0.16	0.09	0.05	0.15	0.11	0.19	0.17	0.15	0.11	0.26
8	0.52	0.63	0.42	0.79	0.16	0.59	0.58	0.36	0.15	0.52	0.38	0.26	0.33	0.38	0.15	0.32	0.28	0.42	0.48	0.57	0.23	0.22
9	0.69	0.30	0.20	0.26	0.07	0.25	0.24	0.21	0.30	0.23	0.24	0.15	0.15	0.15	0.08	0.29	0.14	0.23	0.23	0.22	0.31	0.22
10	0.78	0.03	0.15	0.04	0.01	0.06	0.02	0.04	0.11	0.04	0.01	0.18	0.03	0.01	0.05	0.02	0.05	0.02	0.01	0.03	0.02	0.22
11	0.35	0.21	0.19	0.27	0.06	0.25	0.17	0.14	0.11	0.20	0.14	0.11	0.12	0.11	0.07	0.33	0.14	0.20	0.18	0.21	0.21	0.60
12	0.35	0.63	0.41	0.52	0.15	0.52	0.57	0.36	0.19	0.59	0.33	0.46	0.26	0.41	0.16	0.32	0.26	0.33	0.38	0.36	0.44	0.35
13	0.61	0.16	0.12	0.21	0.06	0.23	0.16	0.16	0.12	0.24	0.12	0.21	0.09	0.10	0.05	0.59	0.10	0.15	0.15	0.15	0.17	0.46
14	0.87	0.31	0.21	0.27	0.08	0.28	0.24	0.19	0.14	0.27	0.17	0.20	0.15	0.15	0.07	0.33	0.16	0.19	0.20	0.18	0.27	0.22
15	0.69	0.98	0.54	0.94	0.19	0.75	0.65	0.53	0.16	0.67	0.42	0.41	0.34	0.48	0.20	0.30	0.39	0.42	0.52	0.60	0.70	0.37
16	0.69	0.82	0.49	0.81	0.15	0.70	0.49	0.44	0.20	0.59	0.39	0.52	0.31	0.44	0.19	0.28	0.35	0.39	0.43	0.63	0.68	0.24
17	0.78	0.34	0.35	0.59	0.19	0.46	0.66	0.26	0.21	0.44	0.50	0.19	0.36	0.33	0.12	0.20	0.35	0.43	0.43	0.41	0.65	0.37
18	0.69	0.01	0.06	0.03	0.01	0.08	0.01	0.09	0.11	0.07	0.01	0.14	0.03	0.01	0.05	0.02	0.04	0.01	0.01	0.02	ND	0.22
19	0.61	0.56	0.38	0.65	0.15	0.55	0.46	0.33	0.14	0.53	0.35	0.35	0.32	0.34	0.14	0.36	0.26	0.38	0.45	0.44	0.55	0.31
20	1.04	0.07	0.17	0.13	0.08	0.18	0.23	0.12	0.83	0.16	0.16	0.11	0.15	0.07	0.06	0.26	0.14	0.18	0.14	0.09	0.14	6.53
Mean	0.67	0.35	0.28	0.38	0.09	0.39	0.29	0.22	0.18	0.30	0.22	0.20	0.18	0.19	0.10	0.36	0.19	0.23	0.24	0.27	0.32	0.67

The results of the Igeo index are shown in (Table 3). According to the classification, the values of all the elements in this study indicate that the sediments were in the “lack of contamination” to “moderate contamination” groups because the Igeo for all these elements was a between zero and one [36].

Statistical Analysis Oxides Concentration

The concentrations of oxides of the elements (in percent) in the sequences of Imamhassan stratigraphical section, and their

mean, minimum, maximum and standard deviation values in comparison with their values in the Earth’s crust are presented in (Table 4).

Table 4. Major oxide concentration of the sediments of Emamhasan section

Sample	SiO ₂	Al ₂ O ₃	Fe ₂ O ₃	CaO	MgO	Na ₂ O	K ₂ O	P ₂ O ₅	TiO ₂
1	33.7	9.6	5.3	20.3	4	0.5	2.5	0.1	0.7
2	42.9	11.9	8.1	12.2	6	0.6	2.7	0.1	0.9
3	36.3	10.8	5.9	18.1	3.5	0.6	2.7	0.1	0.7
4	45.5	12.7	8.1	6.1	11.8	0.6	2.3	0.2	1
5	41.6	12.4	8.4	12.4	6.9	0.6	2.6	0.1	1
6	19.2	6.2	3.7	35.8	2	0.3	1.4	0.1	0.5
7	36	10.3	6.5	20	4.1	0.6	1.9	0.1	0.8
8	39.3	10.5	5.5	20	4.1	0.9	0.2	0.1	0.8
9	34.1	10.1	4.5	23.6	2.9	0.6	2.1	0.1	0.6
10	38.9	11.2	7.9	16.2	4.3	0.7	2.5	0.1	0.9
11	33.7	10	6.2	22.8	3.4	0.6	2.2	0.1	0.8
12	34.8	10.4	7	17.7	5.2	0.6	2.3	0.1	0.9
13	17.5	4.9	5.9	26.2	10.5	0.3	1.1	0.1	0.4
14	15.2	4.7	6.6	26.1	10.8	0.4	1	0.1	0.4
15	34.1	9.8	4.9	21.5	6.3	0.6	1.9	0.1	0.7
16	41.4	13	7.1	14.1	3.1	0.6	2.9	0.1	1
17	34	10.1	8.1	16.9	7.9	0.5	2	0.1	0.8
18	38.7	11.6	7.7	16.1	4.8	0.6	2.7	0.1	0.9
19	36.6	9	4.7	27.3	2.1	1.2	1.7	0.1	0.9
20	36.8	11.6	5.9	18.6	4	0.6	2.2	0.1	0.8
21	42.3	12.7	8.8	13.7	3.2	0.5	3.3	0.1	0.9
22	44.5	13.8	8.4	10.8	4.4	0.7	3.4	0.1	0.8
23	33.5	10.1	5.6	20.8	5.7	0.6	1.9	0.1	0.7
24	31.5	9.1	6.9	27.6	3.5	0.9	1.4	0.1	1.2
Mean	35.0	10.2	6.5	19.3	5.1	0.61	2.1	0.10	0.79
Min	15.2	4.7	3.7	6.1	2	0.3	0.2	0.1	0.4
Max	45.5	13.8	8.8	35.8	11.8	1.2	3.4	0.2	1.2
SD	7.8	2.3	1.4	6.4	2.6	0.1	0.7	0.02	0.1
Crust Values	61.5	15.1	6.28	5.5	3.7	3.2	2.4	0.18	0.68

The concentrations of the oxides of the elements are presented in (Table 4). The amount of SiO₂ (mean value of 35 percent), Al₂O₃ (mean value of 10.27 percent), Fe₂O₃ (6.57 percent), Na₂O (mean value of 0.61 percent), K₂O (mean value of 2.12 percent), P₂O₅ (mean value of 0.10 percent) were in the range of crustal concentration. However, the levels of CaO (19.37), MgO

(5.18) and TiO₂ (0.79) were higher than the crust values. The high values of CaO are due to the presence and repetition of calcareous dolomitic units in these sequences; even, based on XRD analysis results (Figures 4 and 5), these values are high in some marl units. So that there is a high percentage of calcium carbonate in all of them.

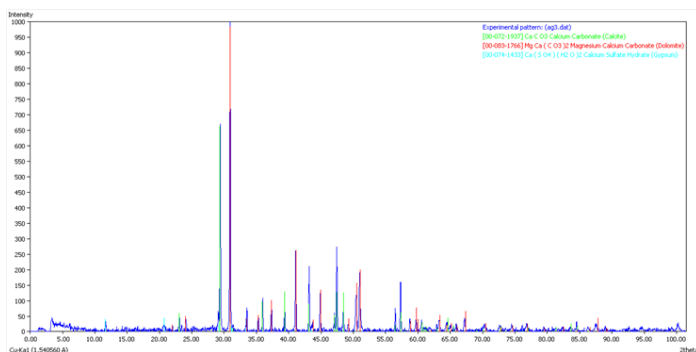


Figure 4: XRD analysis of calcareous, dolomitic units

Calcium can be found along with carbonates, phosphates, and in aluminosilicate minerals in sedimentary rocks (Kuroda et al. 2005). In black shales, calcium is found in various forms and with different compositions, especially in the form of calcite or dolomite. However, it can be found in silicate minerals such as anorthites. In black shales, low levels of CaO substantially prove carbonate deficiency in the environment. This calcium-free may be due to the Paleogeographical location of the relevant sedimentary basins or it may be due to the substitution of Sr for Ca (Burgan et al. 2008).

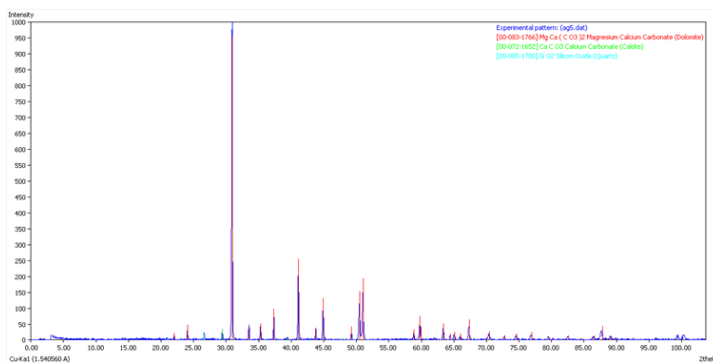


Figure 6: XRD analysis of dolomitic units

MgO is commonly found in light siliciclastic sediments. This compound is also a major component of seawater ions. This compound is mainly found due to cation exchange in dolomites. Burgan et al. (2008) showed that high amounts of MgO and CaO depletion caused by the weathering effects are related to the organic matter origin (Burgan et al. 2008).

Regarding the TiO₂, which can often be found in the composition of clastic sediments (in the study of marl section), it is believed that Ti is a better mediator for the internal flux of clastic sediments

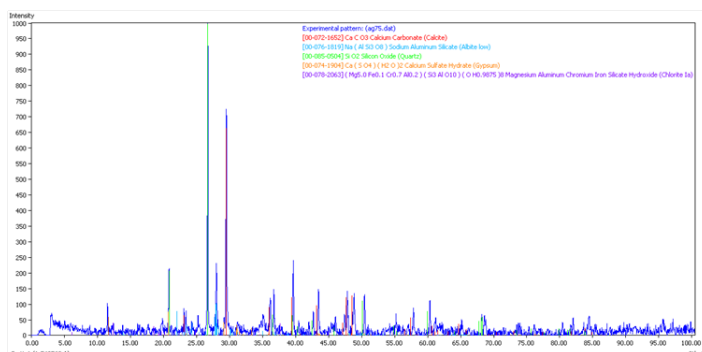


Figure 5: XRD analysis in Marl units

Lipinski et al. (2003) also showed that carbonate percentages decreased due to dilution effects in TOC-rich sediments (Lipinski et al. 2003).

MgO values are also high in dolomitic units that contain calcium-magnesium carbonates. The XRD analysis graph also confirms the high values of this oxide. These graphs also show that even in some marl units, there is a high value of MgO (Figures 6, and 7).

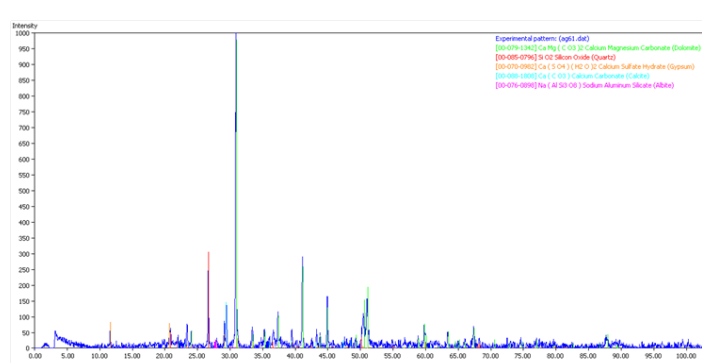


Figure 7: XRD analysis of Marl units

compared to the Al, since the total concentrations of Al can have partially autogenous or biogenic origin (Wei et al., 2003). The relative amounts of Al, Si, k and Ti in shales are mainly controlled by weathering, transport, and decomposition processes (Burgan et al. 2008)

Trace elements Concentration

The concentrations of different elements, mean, minimum, maximum and standard deviation of these elements in the sequences of Imamhassan stratigraphical section were shown in (Table 5). Shale average, Upper crust; [33, 41].

Table 5: Trace element Concentrations in PPM

Sample	Ti	Cs	Ga	Hf	La	Nb	Nd	Rb	Sb	Sc	Sm	Ta	Tb	Th	Tl	U	W	Y	Yb	Zr	Fe	Cd
1	4196	0.18	4.4	0.14	1.6	16.46	0.9	7.8	0.38	0.7	0.13	0.07	0.05	0.20	0.10	0.74	0.18	0.6	0.07	5.3	N.D.	0.46
2	4196	0.35	5.0	0.16	4.3	1.58	1.8	11.8	0.29	1.0	0.38	0.11	0.05	0.48	0.10	4.10	0.17	1.7	0.17	7.8	2098	0.23
3	5994	0.22	10.3	0.17	3.2	1.28	1.6	11.8	0.14	1.1	0.39	0.07	0.06	0.39	0.10	8.85	0.15	1.8	0.19	6.2	1398	0.10
4	5994	4.81	11.2	3.20	18.0	8.12	16.1	74.6	0.37	8.7	3.11	0.19	0.41	5.54	0.34	2.44	0.74	13.2	1.44	112.3	37070	0.20
5	2997	6.55	12.2	3.89	20.2	10.55	15.6	93.4	0.27	10.8	3.29	0.21	0.45	6.42	0.34	1.78	1.16	15.1	1.83	143.3	41266	0.20
6	4795	0.96	4.3	0.69	8.4	5.27	6.7	22.4	0.26	2.4	1.44	0.05	0.20	1.37	0.10	1.02	0.32	7.4	0.57	24.9	8393	0.10
7	4795	0.93	4.3	0.79	12.0	3.38	9.5	22.9	0.35	2.6	1.88	0.12	0.24	1.70	0.10	0.82	0.31	7.4	0.67	35.4	7693	0.12
8	3596	4.76	11.8	3.32	22.6	9.71	20.9	74.9	0.34	10.2	3.65	0.31	0.49	6.91	0.32	1.79	0.76	16.5	1.86	136.2	16087	0.10
9	4795	2.22	5.8	1.11	9.6	4.12	8.6	44.9	0.67	4.4	2.33	0.18	0.22	2.68	0.17	1.60	0.39	9.0	0.90	52.3	21682	0.10
10	5395	0.19	4.4	0.17	1.1	1.05	0.6	8.9	0.25	0.7	0.14	0.22	0.05	0.23	0.10	0.09	0.14	0.7	0.05	7.4	1398	0.10
11	2398	1.59	5.4	1.15	7.9	4.16	6.2	30.0	0.25	3.9	1.32	0.14	0.19	1.99	0.14	1.82	0.38	7.8	0.71	50.6	14688	0.27
12	2398	4.74	11.7	2.19	21.3	8.58	20.4	76.0	0.43	11.6	3.17	0.56	0.40	7.29	0.33	1.78	0.70	12.8	1.49	85.4	31474	0.16
13	4196	1.18	3.38	0.87	8.89	3.81	5.69	34.1	0.28	4.60	1.13	0.26	0.14	1.80	0.10	3.28	0.28	5.85	0.59	36.0	11890	0.21
14	5994	2.34	6.1	1.15	10.5	4.66	8.5	39.2	0.31	5.3	1.67	0.24	0.23	2.72	0.14	1.83	0.44	7.6	0.76	44.2	18884	0.10
15	4795	7.33	15.4	3.93	25.6	12.35	23.3	111.7	0.37	13.1	4.02	0.49	0.51	8.67	0.41	1.67	1.05	16.6	2.02	144.6	49659	0.17
16	4795	6.12	13.8	3.38	21.2	11.59	17.7	92.7	0.46	11.6	3.74	0.62	0.46	7.88	0.40	1.55	0.94	15.4	1.67	150.4	48261	0.11
17	5395	2.56	9.9	2.48	26.6	7.67	23.6	55.3	0.47	8.6	4.83	0.23	0.54	6.01	0.25	1.14	0.93	16.6	1.69	99.5	46162	0.17
18	4795	0.10	1.84	0.11	0.88	1.36	0.46	18.8	0.25	1.31	0.06	0.16	0.05	0.14	0.10	0.13	0.11	0.4	0.05	3.72	N.D.	0.10
19	4196	4.19	10.9	2.74	20.8	9.04	16.4	69.5	0.32	10.3	3.36	0.43	0.49	6.10	0.30	2.01	0.70	15.0	1.77	106	39168	0.14
20	7193	0.55	4.95	0.56	11.4	2.90	8.14	24.7	1.86	3.14	1.51	0.13	0.23	1.28	0.12	1.47	0.38	6.83	0.53	22.7	9792	2.94
Mean	4645	2.59	7.85	1.61	12.8	6.38	10.62	46.3	0.42	5.81	2.08	0.24	0.27	3.49	0.20	2.00	0.51	8.91	0.95	63.7	22615	0.30
Min	2398	0.10	1.8	0.11	0.9	1.05	0.5	7.8	0.14	0.7	0.06	0.05	0.05	0.14	0.10	0.09	0.11	0.4	0.05	3.7	ND	0.10
Max	7193	7.33	15.4	3.93	26.6	16.46	23.6	111.7	1.86	13.1	4.83	0.62	0.54	8.67	0.41	8.85	1.16	16.6	2.02	150.4	49659	2.94
S D	1212	2.39	4.03	1.37	8.5	4.31	7.95	32.3	0.35	4.31	1.48	0.16	0.17	2.97	0.11	1.86	0.33	5.88	0.69	53.1	17147	0.62
Crust	5700	3	15	3	30	20	28	90	0.2	22	6	2	0.9	9.6	0.45	2.7	1.5	33	3	165	56300	0.2
Shale	4600	5	19	2.8	92	11	24	140	1.5	13	6.4	0.8	1	12	1.4	3.7	1.8	26	2.6	160	47200	0.3

Considering the results of (Table 5), the mean value of Sb (0.42 ppm) is higher than that of the earth's crust (0.2 ppm). In addition, cadmium shows a higher concentration in the earth's crust, so that its concentration in the studied sediments had a mean value of (0.30 ppm), but its concentration in the crust was (0.2) ppm. The Sb antimony element is a metallic one that has the same chemical behavior as arsenic and is found under oxic conditions in two stable forms Sb (III) and Sb (V) [42]. At the limit of redox reactions, a resuscitation step is required to stabilize the Sb resuscitation media and remain unchanged [39].

Cadmium (Cd) is an important nutrient for phytoplankton. This element is found in form of (cd (II) or Cd + Cl) in the water column under oxic and sub-oxic conditions and is combined with organic matter and acts as the main carrier to the seabed. it much easier forms cadmium sulfide (Cds) in the presence of H₂S compared to FeS, forms separate sulfide phases rather than being combined with FeS [43, 44]. Because cadmium can bind to organic matter through

the biological cycle, the Cd/Al ratio is used as an old indicator of biological productivity in the field of geological records [39]. FeS may be combined with cadmium or absorbs some of it; in this case, it is necessary to determine to what extent the concentration of cadmium in the sediments is related to organic matter or pyrite, and this is identified by analyzing the correlations between Cd/Al, TOC/Al, and Si/Al [43, 45].

The element of Ti (with an average 4645 ppm) also showed a higher value compared to the shale (4600 ppm), which is discussed in the section of the concentration of elemental oxides (related to TiO₂). For the other elements studied, the concentration was in their range in the crust and shale.

Trace elements Correlation

The correlation between the elements in the sequences of Imamhassan stratigraphical section was presented in (Table 6).

Table 6: Pearson's correlation coefficient of Trace metal concentrations in Emamhasan section

	Ti	Cs	Ga	Hf	La	Nb	Nd	Rb	Sb	Sc	Sm	Ta	Tb	Th	Tl	U	W	Y	Yb	Zr	Cd	
Ti	1																					
Cs	-0.302	1																				
Ga	-0.153	0.891**	1																			
Hf	-0.257	0.971**	0.880**	1																		
La	-0.175	0.859**	0.819**	0.912**	1																	
Nb	-0.317	0.653**	0.596**	0.647**	0.562**	1																
Nd	-0.188	0.856**	0.820**	0.902**	0.992**	0.571**	1															
Rb	-0.267	0.990**	0.878**	0.972**	0.895**	0.625**	0.891**	1														
Sb	0.466*	-0.092	-0.097	-0.077	0.092	-0.072	0.070	-0.035	1													
Sc	-0.303	0.961**	0.877**	0.956**	0.939**	0.626**	0.936**	0.978**	-0.025	1												
Sm	-0.147	0.842**	0.798**	0.903**	0.984**	0.549*	0.980**	0.880**	0.074	0.914**	1											
Ta	-0.278	0.754**	0.694**	0.675**	0.684**	0.463*	0.694**	0.774**	-0.040	0.820**	0.647**	1										
Tb	-0.167	0.872**	0.819**	0.934**	0.987**	0.585**	0.978**	0.901**	0.072	0.938**	0.984**	0.664**	1									
Th	-0.285	0.957**	0.898**	0.959**	0.951**	0.643**	0.956**	0.971**	-0.041	0.992**	0.935**	0.811**	0.950**	1								
Tl	-0.252	0.971**	0.922**	0.962**	0.880**	0.666**	0.886**	0.972**	-0.045	0.962**	0.867**	0.788**	0.895**	0.972**	1							
U	0.138	-0.111	0.210	-0.128	-0.147	-0.262	-0.175	-0.128	-0.179	-0.125	-0.177	-0.159	-0.196	-0.134	-0.109	1						
W	-0.223	0.936**	0.858**	0.967**	0.934**	0.643**	0.916**	0.945**	0.019	0.940**	0.929**	0.645**	0.943**	0.944**	0.926**	-0.161	1					
Y	-0.218	0.884**	0.808**	0.939**	0.978**	0.564**	0.968**	0.911**	0.054	0.939**	0.982**	0.653**	0.988**	0.948**	0.887**	-0.167	0.940**	1				
Yb	-0.269	0.930**	0.857**	0.968**	0.972**	0.607**	0.963**	0.950**	-0.013	0.970**	0.966**	0.698**	0.982**	0.974**	0.930**	-0.136	0.957**	0.987**	1			
Zr	-0.274	0.964**	0.875**	0.992**	0.916**	0.643**	0.905**	0.968**	-0.064	0.957**	0.915**	0.710**	0.937**	0.965**	0.960**	-0.139	0.961**	0.948**	0.970**	1		
Cd	0.448*	-0.216	-0.188	-0.193	-0.063	-0.121	-0.099	-0.177	0.941**	-0.164	-0.118	-0.187	-0.083	-0.195	-0.180	-0.075	-0.104	-0.110	-0.165	-0.199	1	

**Correlation is significant at the 0.01 level.

*Correlation is significant at the 0.05 level.

Based on these results (Table 6), Ti had a significant positive correlation with Sb and Cd and a weak positive correlation with U; it had also a negative correlation with other elements.

The element of Cs had a strong positive and significant correlation with Ga, Hf, La, Nb, Nd, Rb, Sc, Sm, Ta, Tb, Th, Tl, W, Y, Yb and Zr but it showed a negative correlation with Sb, U and Cd elements.

Ga had a positive significant correlation with Hf, La, Nb, Nd, Rb, Sc, Sm, Ta, Tb, Th, Tl, W, Y, Yb and Zr; it showed a weak positive correlation with U while it had a weak negative correlation with Sb and Cd.

Hf showed a strong positive correlation with La, Nb, Nd, Rb, Sc, Sm, Ta, Tb, Th, Tl, W, Y, Yb and Zr, whereas it had a weak negative correlation with Sb, U and Cd.

La had a significant positive correlation with Nb, Nd, Rb, Sc, Sm, Ta, Tb, Th, Tl, W, Y, Yb and Zr and had a weak positive correlation with Sb but it had a negative correlation with U and Cd.

Nb had a strong positive correlation with Nd, Rb, Sc, Sm, Ta, Tb, Th, Tl, W, Y, Yb and Zr but it had a weak negative correlation with Sb, U and Cd.

Rb was positively correlated with Sc, Sm, Ta, Tb, Th, Tl, W, Y, Yb and Zr, while it was negatively correlated with Sb, U and Cd.

Sb had a strong positive correlation with Cd, whereas it had a weak positive correlation with Sm, Tb, W and Y. This element had a weak negative correlation with Sc, Ta, Th, Tl, U, Yb and Zr.

Sc had a strong positive correlation with Sm, Ta, Tb, Th, Tl, W, Y, Yb and Zr and a weak negative correlation with U and Cd.

Sm had a significant positive correlation with Ta, Tb, Th, Tl, W, Y, Yb and Zr, whereas it had a weak negative correlation with U and Cd.

Ta had a strong positive correlation with Tb, Th, Tl, W, Y, Yb and Zr and had a weak negative correlation with U and Cd.

Tb had a strong positive correlation with Th, Tl, W, Y, Yb and Zr, whereas it had a weak negative correlation with U and Cd.

Th had a significant positive correlation with Tl, W, Y, Yb and Zr and showed a weak negative correlation with U and Cd.

Tl had a strong positive correlation with W, Y, Yb and Zr and a weak negative correlation with U and Cd.

U had a negative correlation with W, Y, Yb, Zr and Cd and had no positive correlation with any of the elements.

W showed a strong positive correlation with Y, Yb and Zr and a negative correlation with Cd.

Y had a positive correlation with Yb and Zr but it was negatively correlated with Cd.

Yb had a strong positive correlation with Zr but it had a weak negative correlation with Cd.

Finally, Zr showed a weak negative correlation with Cd.

According to these results, it can be said that Cs, Ga, Hf, La, Nb, Nd, Rb, Sc, Sm, Ta, Tb, Th, Tl, W, Y, Yb and Zr show a significant positive correlation with each other. They probably have mainly originated from common bedrock [13, 22, 46, 47]. In addition, this may be due to similarities in the geochemical behavior of these elements [48].

Element of U did not show a significant positive correlation with other elements, which could indicate that uranium was derived from lithogenic sources [49].

The Ti element showed a strong positive correlation with Sb and Cd, indicating that these three elements may have originated from similar source or have similar geochemical behavior [13,22, 46-48].

The three elements Sb, U and Cd showed a negative correlation with most of the elements that may indicate different origins of these three elements [49, 50].

Cluster Analysis

The results of cluster analysis of the elements present in the sequences of the Imamhassan stratigraphical section are shown in (Figure 8).

Dendrogram using Average Linkage (Between Groups)

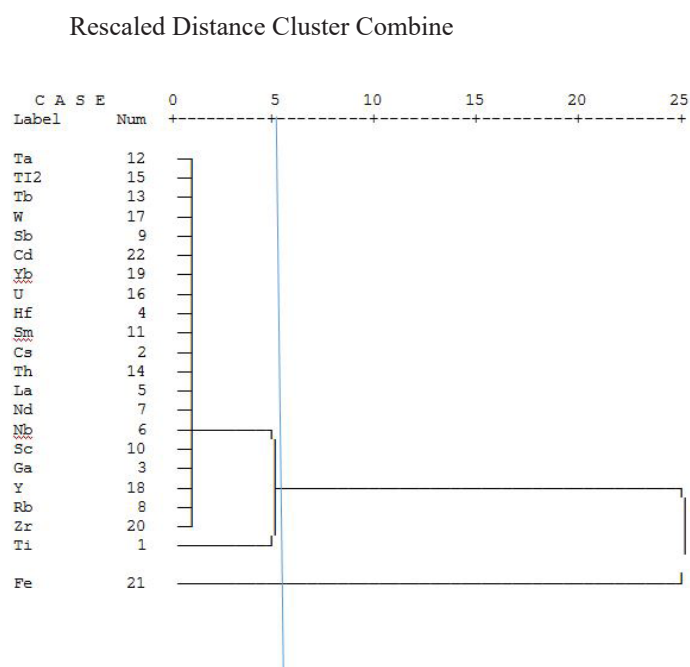


Figure 8: Hierarchical dendrogram for trace metals in Emamhasan section using the nearest neighbour method and Pearson correlation with z standardization.

(Figure 8) shows the results of the cluster analysis, which according to this analysis, classified three distinct groups. The Ti and Fe elements are classified in one group and the Fe element shows the most difference with the other elements. Each Ti and Fe were placed in a separate cluster, which could be due to their different geochemical origin or behavior compared to the other elements.

Principal Component Analysis (PCA)

Principal Component Analysis (PCA) was used to identify the source of metals in the sediments of the Imamhassan section. The analysis was performed by SPSS software version 17 and the

results were presented in (Table 7). The percentages of cumulative variances deduced from the first three components and the values of the three principal components for maximum variance in the sequences of the Imamhassan stratigraphical section are presented in (Table 7).

Table 7: The result of principal component analysis for sediment in Emamhasan section

Variables	Component		
	1	2	3
Ti	-.311	.589	.435
Cs	.955	-.089	.071
Ga	.870	-.114	.421
Hf	.974	-.036	.046
La	.955	.153	-.040
Nb	.982	-.033	-.012
Nd	.948	.126	-.057
Rb	.974	-.021	.065
Sb	-.076	.962	.018
Sc	.985	-.013	.021
Sm	.944	.137	-.071
Ta	.748	-.073	-.012
Tb	.961	.146	-.061
Th	.993	-.024	.021
TI2	.968	-.028	.124
U	-.304	-.311	.843
W	.964	.071	.014
Y	.966	.101	-.093
Yb	.987	.018	-.031
Zr	.977	-.036	.018
Fe	.926	.061	.038
Cd	-.205	.911	.096

Extraction Method: Principal Component Analysis.
a. 3 components extracted.

Analysis of principal component analysis (Table 7) shows that the first three components account for more than 90% of the variance, of which the first component is 74% and the second component is 10% and the third component is 5% of the cumulative variance. The remaining 10% of the variance is related to other components. Based on these results, Cs, Hf, La, Nb, Nd, Rb, Sc, Sm, Tb, Th, Ti, W, Y, Yb, Zr and Fe in the first component, Sb and Cd in the second component and U in the third component, had the most impact. As shown in (Table 7), the first component accounted for 74% of the variance, and most of the elements are in the first component and have high values of positive correlation, which may be the reason for this fact that most of these elements have the same origin such as the same material of the bedrock. showed

that the elements in a component have a common origin [46]. High amounts of Ti and Fe can also indicate bed rock weathering in the deposits. Regarding the second component, Sb and Cd had a positive correlation, indicating the common origin of these two elements. The third component had a high positive correlation with U indicating a different origin for this element.

Conclusions

The investigation of geochemical properties of Gachsaran Formation sequences in the study area showed that Cs, Hf, La, Nb, Nd, Rb, Sc, Sm, Tb, Th, Tl, W, Y, Yb, Zr and Fe had the highest significant positive correlation with each other. It shows the same origin of these elements. Sb and Cd also showed a significant positive correlation with the second component, which may indicate the same origin of these two elements. The element of U also showed a high positive correlation with the third component, indicating a different source of this element compared to other elements. According to the contamination factor (CF), Cd and Sb elements showed moderate contamination; based on enrichment factor (EF), Cs, Ga and Rb elements revealed moderate contamination, and Tl, Cd, U and Sb elements showed high contamination with anthropogenic origin in sequences of the Gachsaran Formation in the study area. Concentrations of CaO, MgO and TiO₂ were also higher than the mean values in the crust. Also, among the three completely separate groups based on the results of cluster analysis, Ti and Fe elements were grouped separately and the Fe element showed the most difference with other elements.

Availability of data and materials

The datasets used and/or analyzed during the current study are available from the corresponding author on reasonable request.

Competing interests

The authors declare that they have no conflict of interest.

Funding

This was done with the financial support of the Geological Survey of Iran.

Authors' contributions

All authors performed the fieldwork. Behnam conducted the experiments, analyzed the data and wrote the first draft of the manuscript. Mostafa conceived the study and revised the manuscript and data analysis. Anita helped with the contributed to the manuscript revision and analysis. All of the authors drafted, read and approved the final manuscript.

Acknowledgements

This article is extracted from the Ph.D. dissertation of Geology, subdiscipline of Fossil and Stratigraphy, entitled Biostratigraphy and Chemostratigraphy of Gachsaran Formation in Kermanshah. We are also thankful from Dr. Alireza Shahidi and Dr. Fariborz Gharib for helping us to reach the goals of this study.

References

1. Cox, L. R. (1936). Fossil Mollusca from southern Persia (Iran) and Bahrein Island: Memoirs of the Geological Survey of India, v. 22.
2. Pilgrim, G. E. (1910). The geology of the Persian Gulf and the adjoining portions of Persia and Arabia. Sold at the Office of the Geological Survey of India.
3. Richardson, R. K. (1924). The Geology and Oil Measures of South-west Persia, &c. W. Speaight and Sons.
4. Strong, M. W. (1937, June). Micropetrographic methods as an aid to the stratigraphy of chemical deposits. In 2nd World Petroleum Congress. OnePetro.
5. Furon, R. (1941). Geologie du Plateau Iranien (Perse, Afghanistan, Belouchistan). Éditions du Muséum.
6. Watson, S., (1960). a-Revision of the lower Fars key beds in the Gachsaran field. IOOC Report.
7. James, G. A., & Wynd, J. G. (1965). Stratigraphic nomenclature of Iranian oil consortium agreement area. AAPG bulletin, 49(12), 2182-2245.
8. Setudehnia, A. (1972). Iran du Sud-Ouest: Lexique Strat. Internat. Cen. Nat. Rech. Sci. Pari, III, Asia 9b, 289-376.
9. Daneshian, J., Norouzi, N. B. D. A. S., BAGHBANI, D., & AGHANABATI, S. (2011). Biostratigraphy oligocene and lower miocene deposits (pabdeh, asmari, gachsaran and mishan formations) on the basis foraminifera in southwest of jahrom, interior fars. earth sciences. Survey India, Paleont. Indica, ns, 166, 57-83.
10. Amiri Bakhtiar, H., & Nourainejad, K. (2014). Zagros stratigraphic review: Gachsaran formations. scientific monthly journal of exploration and production of oil and gas. Environmental Nanotechnology, Monitoring & Management, 111, 40-45.
11. Khan, M. Z. H., Hasan, M. R., Khan, M., Aktar, S., & Fatema, K. (2017). Distribution of heavy metals in surface sediments of the Bay of Bengal Coast. Journal of Toxicology, 2017.
12. Rainbow, P. S. (2007). Trace metal bioaccumulation: models, metabolic availability and toxicity. Environment international, 33(4), 576-582.
13. Yang, Y., Chen, F., Zhang, L., Liu, J., Wu, S., & Kang, M. (2012). Comprehensive assessment of heavy metal contamination in sediment of the Pearl River Estuary and adjacent shelf. Marine Pollution Bulletin, 64(9), 1947-1955.
14. Gümğüm, B., Tez, Z., & Gülsün, Z. (1994). Heavy metal pollution in water, sediment and fish from the Tigris River in Turkey. Chemosphere, 29(1), 111-116.
15. Potra, A., Dodd, J. W., & Ruhl, L. S. (2017). Distribution of trace elements and Pb isotopes in stream sediments of the Tri-State mining district (Oklahoma, Kansas, and Missouri), USA. Applied Geochemistry, 82, 25-37.
16. Sahoo, P. K., Tripathy, S., Panigrahi, M. K., & Equeenuddin, S. M. (2014). Geochemical characterization of coal and waste rocks from a high sulfur bearing coalfield, India: Implication for acid and metal generation. Journal of geochemical Exploration, 145, 135-147.
17. Adamu, C. I., Nganje, T. N., & Edet, A. (2015). Heavy metal

- contamination and health risk assessment associated with abandoned barite mines in Cross River State, southeastern Nigeria. *Environmental Nanotechnology, monitoring & management*, 3, 10-21.
18. Purushothaman, P., & Chakrapani, G. J. (2007). Heavy metals fractionation in Ganga River sediments, India. *Environmental monitoring and assessment*, 132(1), 475-489.
19. Milenkovic, N., Damjanovic, M., & Ristic, M. (2005). Study of Heavy Metal Pollution in Sediments from the Iron Gate (Danube River), Serbia and Montenegro. *Polish Journal of Environmental Studies*, 14(6).
20. Tang, W., Shan, B., Zhang, W., Zhang, H., Wang, L., & Ding, Y. (2014). Heavy metal pollution characteristics of surface sediments in different aquatic ecosystems in eastern China: a comprehensive understanding. *PLoS One*, 9(9), e108996.
21. Kuncheva, L. I., Wrench, J., Jain, L. C., & Al-Zaidan, A. S. (2000). A fuzzy model of heavy metal loadings in Liverpool bay. *Environmental Modelling & Software*, 15(2), 161-167.
22. Zarei, I., Pourkhabbaz, A., & Khuzestani, R. B. (2014). An assessment of metal contamination risk in sediments of Hara Biosphere Reserve, southern Iran with a focus on application of pollution indicators. *Environmental monitoring and assessment*, 186(10), 6047-6060.
23. Attia, O. E., & Ghrefat, H. (2013). Assessing heavy metal pollution in the recent bottom sediments of Mabahiss Bay, North Hurghada, Red Sea, Egypt. *Environmental monitoring and assessment*, 185(12), 9925-9934.
24. Pacle Decena, S. C., Sanita Arguelles, M., & Liporada Robel, L. (2018). Assessing Heavy Metal Contamination in Surface Sediments in an Urban River in the Philippines. *Polish Journal of Environmental Studies*, 27(5).
25. Ra, K., Kim, E. S., Kim, K. T., Kim, J. K., Lee, J. M., & Choi, J. Y. (2013). Assessment of heavy metal contamination and its ecological risk in the surface sediments along the coast of Korea. *Journal of Coastal Research*, (65 (10065)), 105-110.
26. Sekabira, K., Origa, H. O., Basamba, T. A., Mutumba, G., & Kakudidi, E. (2010). Assessment of heavy metal pollution in the urban stream sediments and its tributaries. *International journal of environmental science & technology*, 7(3), 435-446.
27. Hu, Y., Liu, X., Bai, J., Shih, K., Zeng, E. Y., & Cheng, H. (2013). Assessing heavy metal pollution in the surface soils of a region that had undergone three decades of intense industrialization and urbanization. *Environmental Science and Pollution Research*, 20(9), 6150-6159.
28. Sutherland, R. A., Tolosa, C. A., Tack, F. M. G., & Verloo, M. G. (2000). Characterization of selected element concentrations and enrichment ratios in background and anthropogenically impacted roadside areas. *Archives of Environmental Contamination and Toxicology*, 38(4), 428-438.
29. Kartal, Ş., Aydın, Z., & Tokaloğlu, Ş. (2006). Fractionation of metals in street sediment samples by using the BCR sequential extraction procedure and multivariate statistical elucidation of the data. *Journal of hazardous materials*, 132(1), 80-89.
30. Ergin, M., Saydam, C., Baştürk, Ö., Erdem, E., & Yörük, R. (1991). Heavy metal concentrations in surface sediments from the two coastal inlets (Golden Horn Estuary and Izmit Bay) of the northeastern Sea of Marmara. *Chemical geology*, 91(3), 269-285.
31. Angelidis, M. O., & Aloupi, M. (1997). Assessment of metal contamination in shallow coastal sediments around Mytilene Greece. *International journal of environmental analytical chemistry*, 68(2), 281-293.
32. Liaghati, T., Preda, M., & Cox, M. (2004). Heavy metal distribution and controlling factors within coastal plain sediments, Bells Creek catchment, southeast Queensland, Australia. *Environment International*, 29(7), 935-948.
33. Turekian, K. K., & Wedepohl, K. H. (1961). Distribution of the elements in some major units of the earth's crust. *Geological society of America bulletin*, 72(2), 175-192.
34. Hakanson, L. (1980). An ecological risk index for aquatic pollution control. A sedimentological approach. *Water research*, 14(8), 975-1001.
35. Forstner, U. (1989). *Lecture notes in earth sciences*.
36. Muller, G. (1969). Index of geoaccumulation in sediments of the Rhine River. *Geojournal*, 2, 108-118.
37. Kuroda, J., Ohkouchi, N., Ishii, T., Tokuyama, H., & Taira, A. (2005). Lamina-scale analysis of sedimentary components in Cretaceous black shales by chemical compositional mapping: Implications for paleoenvironmental changes during the Oceanic Anoxic Events. *Geochimica et Cosmochimica Acta*, 69(6), 1479-1494.
38. Burgan, A. M., Ali, C. A., & Tahir, S. H. (2008). Chemical composition of the Tertiary black shales of West Sabah, East Malaysia. *Chinese Journal of Geochemistry*, 27(1), 28-35.
39. Lipinski, M., Warning, B., & Brumsack, H. J. (2003). Trace metal signatures of Jurassic/Cretaceous black shales from the Norwegian Shelf and the Barents Sea. *Palaeogeography, Palaeoclimatology, Palaeoecology*, 190, 459-475.
40. Wei, G., Liu, Y., Li, X., Shao, L., & Liang, X. (2003). Climatic impact on Al, K, Sc and Ti in marine sediments: evidence from ODP Site 1144, South China Sea. *Geochemical Journal*, 37(5), 593-602.
41. Wedepohl, K. H. (1995). The composition of the continental crust. *Geochimica et cosmochimica Acta*, 59(7), 1217-1232.
42. Elbaz-Poulicheet, F., Nagy, A., & Cserny, T. (1997). The distribution of redox sensitive elements (U, As, Sb, V and Mo) along a river-wetland-lake system (Balaton Region, Hungary). *Aquatic Geochemistry*, 3(3), 267-282.
43. März, C., Beckmann, B., Franke, C., Vogt, C., Wagner, T., & Kasten, S. (2009). Geochemical environment of the Coniacian–Santonian western tropical Atlantic at Demerara Rise. *Palaeogeography, Palaeoclimatology, Palaeoecology*, 273(3-4), 286-301.
44. Tribouillard, N., Algeo, T. J., Lyons, T., & Riboulleau, A. (2006). Trace metals as paleoredox and paleoproductivity proxies: an update. *Chemical geology*, 232(1-2), 12-32.
45. Charriau, A., Lesven, L., Gao, Y., Leermakers, M., Baeyens, W., Ouddane, B., & Billon, G. (2011). Trace metal behaviour in riverine sediments: role of organic matter and sulfides.

-
- Applied Geochemistry, 26(1), 80-90.
46. Chandrasekaran, A., Ravisankar, R., Harikrishnan, N., Satapathy, K. K., Prasad, M. V. R., & Kanagasabapathy, K. V. (2015). Multivariate statistical analysis of heavy metal concentration in soils of Yelagiri Hills, Tamilnadu, India—Spectroscopical approach. *Spectrochimica Acta Part A: Molecular and Biomolecular Spectroscopy*, 137, 589-600.
47. Gupta, S. K., Chabukdhara, M., Kumar, P., Singh, J., & Bux, F. (2014). Evaluation of ecological risk of metal contamination in river Gomti, India: a biomonitoring approach. *Ecotoxicology and Environmental Safety*, 110, 49-55.
48. Pandey, J., & Singh, R. (2017). Heavy metals in sediments of Ganga River: up-and downstream urban influences. *Applied Water Science*, 7(4), 1669-1678.
49. Harikrishnan, N., Ravisankar, R., Chandrasekaran, A., Gandhi, M. S., Kanagasabapathy, K. V., Prasad, M. V. R., & Satapathy, K. K. (2017). Assessment of heavy metal contamination in marine sediments of east coast of Tamil Nadu affected by different pollution sources. *Marine pollution bulletin*, 121(1-2), 418-424.
50. Ravisankar, R., Sivakumar, S., Chandrasekaran, A., Kanagasabapathy, K. V., Prasad, M. V. R., & Satapathy, K. K. (2015). Statistical assessment of heavy metal pollution in sediments of east coast of Tamilnadu using Energy Dispersive X-ray Fluorescence Spectroscopy (EDXRF). *Applied Radiation and Isotopes*, 102, 42-47.

Copyright: ©2022 Sakhavati Behnam. This is an open-access article distributed under the terms of the Creative Commons Attribution License, which permits unrestricted use, distribution, and reproduction in any medium, provided the original author and source are credited.